Proceedings of the ASME 2011 Pacific Rim Technical Conference & Exposition on
Packaging and Integration of Electronic and Photonic Systems
InterPACK2011
July 6-8, 2011, Portland, Oregon, USA

IPACK2011-52268

USE CONDITION CHARACTERIZATION OF PACKAGE COMPONENTS

Leigh Wojewoda
Intel Corporation
Chandler, AZ, USA

Dhanya Athreya
Intel Corporation
Chandler, AZ, USA

Michael J Hill
Intel Corporation
Chandler, AZ, USA

ABSTRACT

Discrete components, such as capacitors and inductors, play an important role in the analysis and design of electronic packages and printed circuit boards. Although the electrical parameters of discrete components are described by manufacturers, the component performance at product operating conditions can vary drastically from the manufacturer's specification. Accurate characterization of discrete package components at operating conditions is essential to understand product operation. This paper will introduce a method to characterize discrete capacitors and inductors while applying multiple operating conditions simultaneously. Several inductor options will be evaluated, including a newly introduced metal composite component.

INTRODUCTION

Discrete components, such as capacitors and inductors, are critical elements in the design of microprocessor packages. However, developing an accurate model of the components can be a challenging task. For example, the capacitance of Multi-Layer Ceramic Capacitors (MLCC) is a strong function of variables such as temperature, DC bias, AC RMS voltage [1,2]. Inductors can be highly dependent on operating frequency and applied current [3,4,5]. Characterization data under a single use condition can sometimes be obtained from component manufacturers [6,7]. However, the full set of data needed to create a representative model may not be available. Other measurement techniques illustrate methods to collect the full data set by utilizing a Vector Network Analyzer, but lack the application of operating conditions [8,9]. This paper will present a measurement technique to simultaneously apply several operating conditions while utilizing a Vector Network

Analyzer to collect the full set of data needed to generate an accurate electrical model for both MLCC and inductors. A measurement fixture and deembedding procedure will be discussed. This paper will presents a custom designed probeable bias tee that allows the application of high current over a broad frequency range.

Also discussed in this paper is the type of model that is used to represent the components. Historically, designers have relied on simple models to represent capacitors and inductors. However, this simple model has been shown to be inadequate for capturing the high frequency behavior of the components [10,11]. This problem is addressed by introducing higher order models to effectively capture the behavior of the component across the frequencies of interest.

OVERVIEW OF COMPONENTS

Figure 1 shows a schematic view and a cross section of an MLCC. MLCCs are composed of many layers of metal electrodes alternating with a very high dielectric constant ceramic. State of the art MLCCs commonly use barium titanate ceramics with a relative dielectric constant in the range of 2000 or greater [12,13]. The thickness of the electrodes and dielectric layers is continually driven smaller by the need to increase capacitance through the addition of layers. Modern MLCCs utilize dielectric and electrode thicknesses in the range of $1 - 2$ μm [12,13].
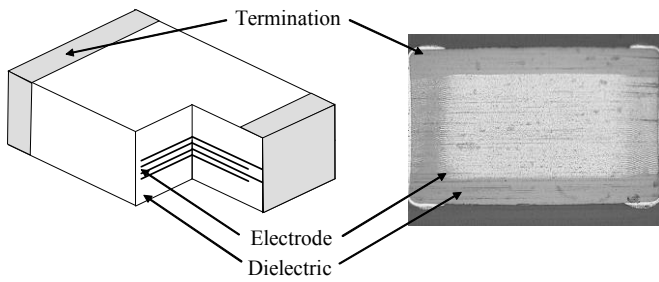
Copyright © 2011 by ASME

Figure 1. MLCC Construction.

Figure 2 shows views of the different types of inductors examined in this paper. The first type of inductor is a wire wound component. A conductor is wound around a core, which can be fabricated from different materials. When a non ferrite material, such as ceramic or plastic, is used for the core, the inductor is commonly referred to as an air core inductor. The core can also be fabricated from magnetic material to increase the inductance of the component [3]. The inductors examined in this paper utilized a bobbin style core rather than a toroidal core. Figure 2 also shows a cross section of a metal composite inductor. Metal composite inductors are formed by embedding the coil inside a composite of resin and iron powder. Recent developments in this area have enabled materials with finer particles. The new materials show improvements in resistance and loss as well as a lower dependence on frequency.
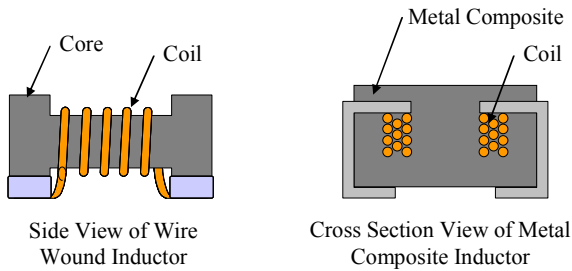

Figure 2. Wire wound and metal composite inductor construction

MEASUREMENT SETUP

The Universal Component Test Vehicle (UCTV) was created by Intel® to measure component parasitics [1,8]. Figure 3 contains an illustration of a test site on the UCTV. The UCTV contains test sites for various component form factors and is manufactured using a build-up process similar to the process used for Intel's microprocessor packages. Each component is measured on a two layer structure, representing a simplified power/ground design. Measurement of the parasitic values includes both component and package contributions. Although the package parasitic values are minimized through design, the parasitics may still become significant when measuring advanced components.

Figure 3(b) shows an enlarged view of a component assembled on the test structure. Each type of component test structure includes a shorted structure, which is illustrated in Figure 3(c) with the soldermask layer removed. The figure of the shorted structure has dashed lines to indicate the positions of the soldermask openings. The shorted structure replicates the component test structure design and is used to deembed the test fixture parasitic values.
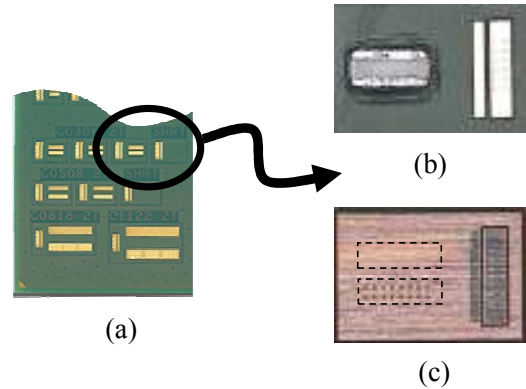

Figure 3. Universal component test vehicle

The measurement setup is illustrated in Figure 4. The setup utilizes an Agilent® 8753 two port Vector Network Analyzer (VNA) measurement [1,8]. The component and test fixture are connected in a shunt configuration between the two ports. Contact to the test fixture is made with 250 um pitch SG/GS RF probes. An SOLT technique is used for calibration. The frequency range of 30 kHz to 3 GHz is typically sufficient to capture the resonance frequency observed in the transmitted S Parameters (S12 or S21). Although all reflected and transmitted S Parameters (S11, S12, S21 and S22) are downloaded from the VNA, only the S21 parameter is used during the data fitting process. The S21 data is used because the measurement sensitivity of S11 and S22 is generally poor for the low impedances typically seen with decoupling capacitors.

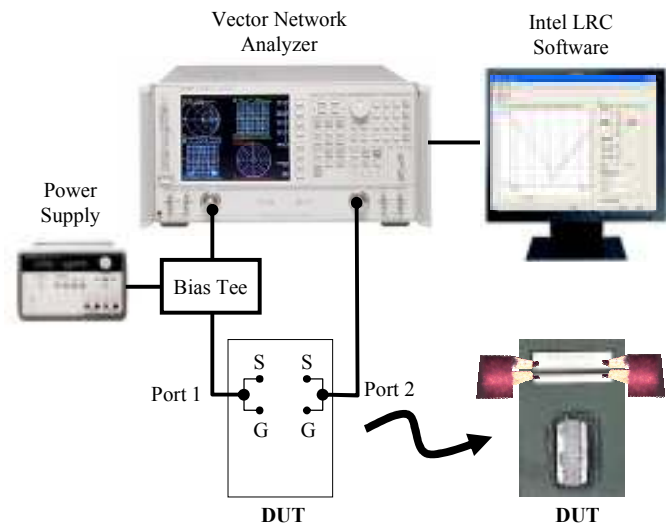Figure 4. Component measurement setup

2   Copyright © 2011 by ASME

A Bias Tee is a high impedance device used to ensure that the power supply connected to the circuit does not introduce artifacts into the measurement. Figure 5 shows a schematic of the implementation of the bias tee in the measurement system.
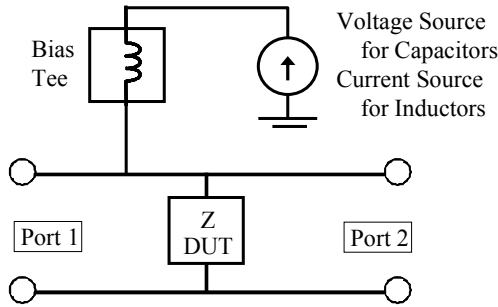

Figure 5. Schematic of bias tee implementation

Bias tees are commonly included as an internal component in VNAs. However, the internal bias tees typically have current limits of 1 Amp or less which may not cover the range of interest for inductor applications. Because of this, an external bias tee was developed, shown in Figure 6. The bias tee can be connected to the RF probes, which allows the use of probeable DUTs, such as the UCTV, and allows currents of up to 5 Amps to be applied.
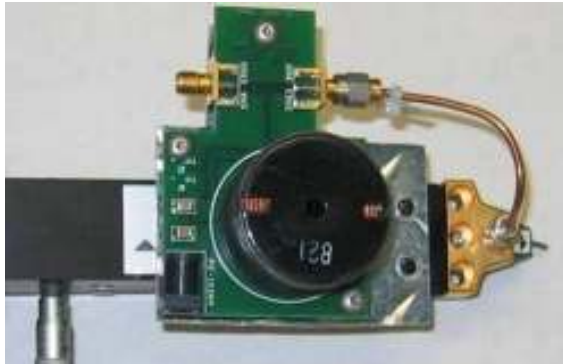

Figure 6. Probeable bias tee

Measurements using the component test structure described earlier consist of contributions from both package and component. Modeling tools can be used to estimate the individual contributions [8]. Another option is to apply a deembedding technique to the measurements.

The deembedding technique makes uses of the test structures shown in Figure 3(b) and (c). For a two port measurement with the shorted structure in a shunt configuration, the impedance of the short can be expressed by the following equation, where both Z_{Short} and S_{21_Short} are complex values [14],

$$Z_{Short} = \frac{-25\Omega \cdot S_{21\_Short}}{S_{21\_Short} - 1}$$

(1)

The impedance of the component assembly may also be calculated using (1). The deembedding procedure is completed by subtracting the impedance of the shorted fixture from the impedance of the component assembly.

$$Z_{Component} = Z_{Component+Fixture} - Z_{Short}$$

(2)

DATA FITTING FOR THE CAPACITOR MODELS

Once the fixture contribution has been deembedded, it is possible to extract the component parasitics from the impedance. An ideal capacitor can be represented as a simple capacitive element in a power delivery model. In reality, all capacitors have a parasitic resistance and inductance associated with them. Figure 7(a) shows a comparison of a measured capacitor impedance to the impedance of an RLC model. Figure 7(b) illustrates the RLC model and values extracted for the 0306 1 µF capacitor.

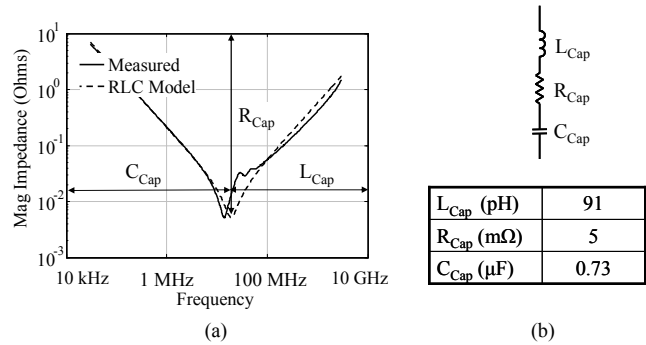| L_{Cap} (pH)	91
R_{Cap} (mΩ)	5
C_{Cap} (µF)	0.73

(a)   (b)

Figure 7. Measured and RLC modeled capacitor response

Until recently, package capacitors were represented using a simple 3-element RLC model. Because of non-ideal behavior, the simple RLC model may not accurately capture the response over the entire frequency range. Some of the limitations of the RLC model can be observed in Figure 7. For example, the resonance frequency is not matched between RLC model and measured data. Also, the simple RLC model may lead to over prediction of inductance. The over prediction of inductance may lead designers to select higher performance or more expensive capacitors than might be required.

Other complex models are described in literature to address these issues [9,10,11]. A 9-element higher order model is presented here which effectively captures the behavior of the capacitor across the frequencies of interest [1]. The higher order model representation is shown in Figure 8, along with the model fit to measured data. The limitations of the RLC model have been addressed with the 9-element model. Both the resonance frequency and high frequency behavior can be matched with the 9-element model.
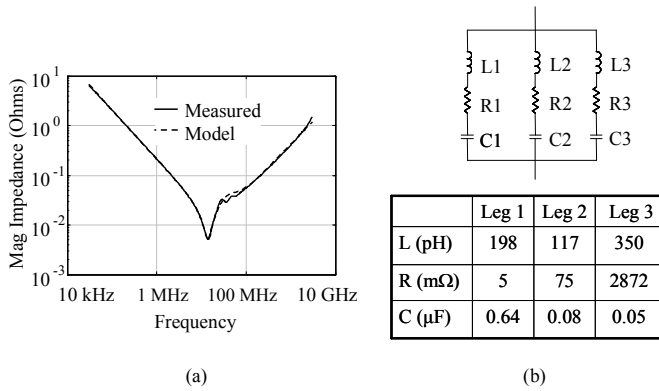
3

Copyright © 2011 by ASME

Figure 8. Measured response and higher order model

The algorithm chosen to generate the higher order model fits both real and imaginary components of the impedance data using a custom optimization technique and has been shown to provide good reproducibility in the presence of measurement noise.

CAPACITOR USE CONDITION MEASUREMENTS

Although the higher order models can be used to accurately capture the component behavior, additional considerations must be taken into account. One important consideration is changes in component response due to use conditions. For capacitors, temperature and voltage conditions strongly impact the capacitance.

Typical MLCCs used in packaging utilize Class II, III and IV dielectrics, which have large dielectric constants. However, MLCCs manufactured with these dielectrics may result in values of capacitance which are lower than the manufacturer's spec value when measured under real world use conditions [1,15]. In state of the art MLCCs, use condition voltages and temperatures usually result in a capacitance decrease.

Each supplier has a proprietary formulation of ceramic used in MLCC manufacturing. The differences in formulation change the sensitivity to temperature and applied voltage. This leads to significant variation between suppliers. The results of use conditions on capacitance measurements are summarized in Figure 9. The measurement setup in Figure 4 was used to provide a DC voltage of 1.2 V. During measurement, the DUT was placed on a thermal chuck and swept through a temperature range. Because of equipment limitations, the RMS voltage was not varied. The applied RMS voltage was estimated to be approximately 0.005V.
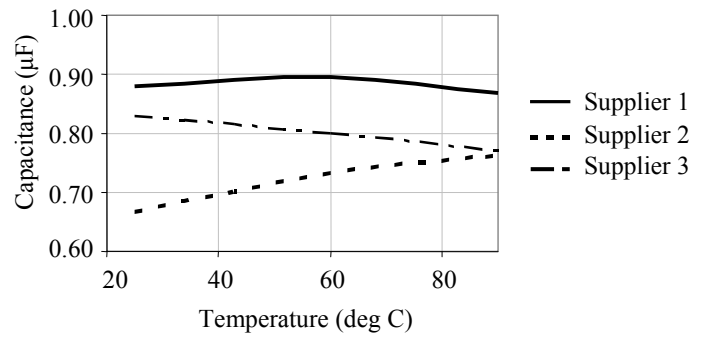

Figure 9. Comparison of 1μF MLCCs from various suppliers using VNA use condition measurements

Figure 9 illustrates the importance of characterizing capacitors at their use condition. Although the capacitors under evaluation are rated as a 1μF component, it can be seen that the value measured at use condition can vary significantly between suppliers.

DATA FITTING FOR THE INDUCTOR MODELS

Inductors can be fabricated from a variety of methods and materials, which can significantly influence the measured response. Three inductors were selected for evaluation. The inductors were selected to have a low frequency inductance of 9 nH, but were constructed by the methods illustrated in Figure 2. The inductor options included a wire wound air core, a wire wound ferrite core and a metal composite construction. Figure 10 describes measured inductance as a function of frequency with no applied current. The wire wound air core shows the largest decrease in effective inductance over the frequency range. The wire wound ferrite inductor shows a relatively small change in inductance and the metal composite inductor shows an almost flat inductance response.
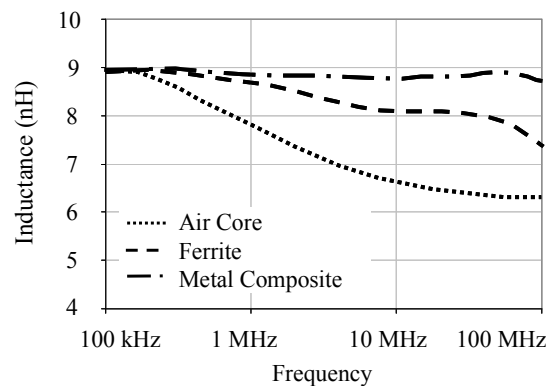

Figure 10. Inductance as a function of frequency for different inductor options

Figure 11 shows the AC resistance frequency response for the same three types of inductors.

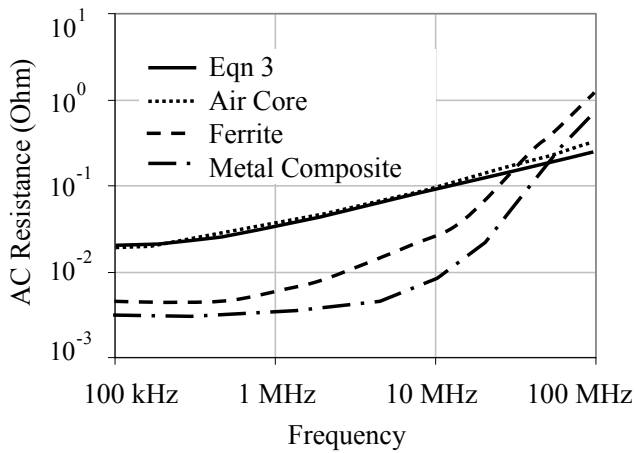4   Copyright © 2011 by ASME

Figure 11. AC resistance for different inductor options

The wire wound air core inductor yields the highest DC resistance. This is because a longer coil is required for an air core inductor to achieve an equivalent resistance to a ferrite inductor. The AC resistance of the air core wire wound inductor can be estimated from the following equation [3],

$$\text{AC Resistance} \approx \frac{\rho}{\delta}\left(\frac{L}{\pi(D-\delta)}\right) \qquad (3)$$

where ρ is copper resistivity, approximately 1.72×10^{-8} Ohm meter, L is the length of the coil, D is the diameter of the coil and δ is the skin depth. Skin depth may be expressed by the following equation [3,4]

$$\delta = \sqrt{\frac{\rho}{\pi\mu_0\mu_R f}} \qquad (4)$$

where μ_0 is the permeability of free space = 1.257×10^{-6} H/m, $\mu_R = 1$ for copper and f is the frequency of interest. The result of (3) is plotted in Figure 11. The results show very good agreement between the measured AC resistance of the air core wire wound inductor and the theoretical prediction. For frequencies above 10 MHz, the ferrite and metal composite inductors yield higher AC resistance than the air core inductors. Ferrite core and metal composite inductors exhibit additional loss mechanisms that can be difficult to predict without detailed knowledge of the core properties [3]. Because of these considerations, it is importance to have a model that captures both inductance and AC resistance over the frequency range of interest.

Figure 12 shows two commonly used inductor models [3]. Model (a) is one of the simplest representations of an inductor. The resistance of Model (a) captures the DC resistance of the coil windings, but does not represent the higher frequency response. Model (b) is another commonly used representation of inductors. There is an additional resistor element in the model, which helps to capture the frequency dependent AC
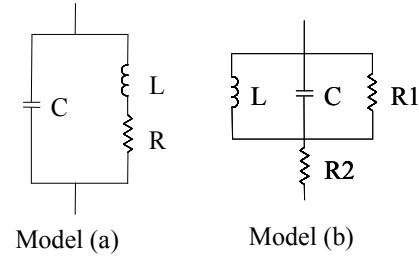
resistance behavior.

Figure 12. Simple inductor models

Figure 13 shows the measured response of the ferrite core wire wound inductor as compared to the two simple inductor models. Figure 13 illustrates the component's inductance and AC resistance response as a function of frequency. It can be seen from the plots that both models generate a relatively flat inductance response. Model (b) captures some of the higher frequency inductance roll off, but neither model captures the low frequency inductance behavior. The AC resistance is also plotted in Figure 13. Model (a) represents only the DC resistance, and therefore, frequency dependent behavior is not captured. Because of the additional resistive element in the model, Model (b) provides a better fit to the AC resistance.
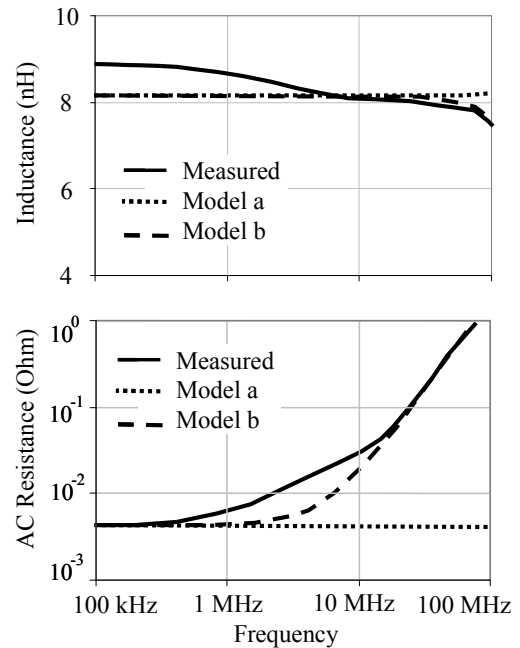

Figure 13. Measured response of ferrite inductor compared to simple inductor models

For many applications, a Model (b) may provide an adequate representation of the inductor. However, there are cases where the simple model does not provide a sufficient fit to the data. For these cases, Figure 14 illustrates a higher order model which can represent both inductance and AC resistance as a function of frequency [5].
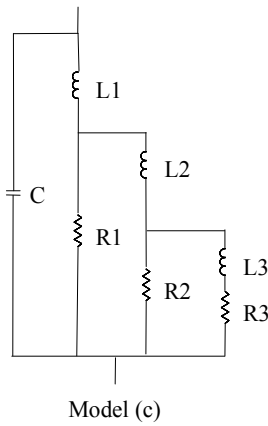
5

Model (c)

Figure 14. Higher order inductor model

Figure 15 illustrates the frequency response of the air core wire wound inductor. The air core inductor showed the largest change in inductance as a function of frequency. The higher order model captures the inductance change better that the simple model. Because of the additional elements in the model, the AC resistance can be very well represented by the higher order model.
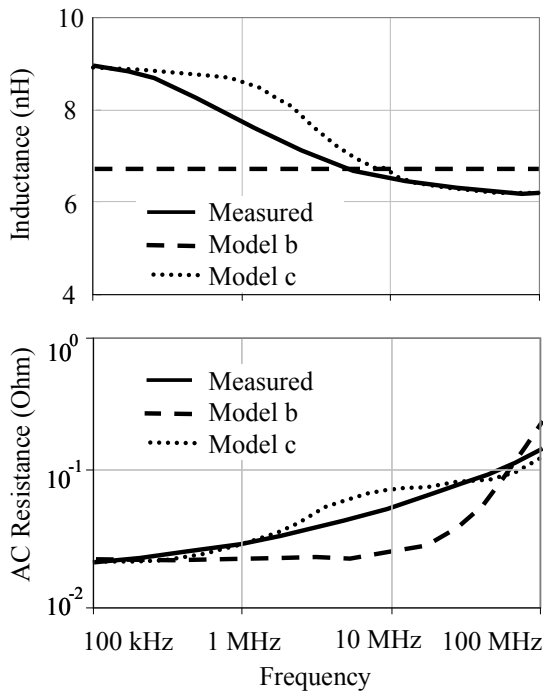

Figure 15. Measured response of air core inductor compared to higher order inductor model

In summary, two simple model options were presented. For certain applications, simple inductor models may be sufficient to represent general inductor characteristics. However, if accurate representation of inductance and AC resistance is required, a higher order model will be necessary.

INDUCTOR USE CONDITION MEASUREMENTS

Similar to capacitors, higher order models can be used to accurately describe an inductor's behavior. However, inductors should also be measured under use condition to achieve meaningful results. Figure 16 describes a summary of inductor behavior under applied current. The measured inductance was recorded at 10 MHz under zero bias current. The current was increased in 1A steps up to 4A. Figure 16 shows the ratio of the inductance measured at zero current to the inductance measured under bias current. Both the air core inductor and the metal composite inductor shows a very flat response with applied current, almost no change was observed. The ferrite core inductor showed the largest change in inductance, with a decrease of almost 8%. Figure 16 demonstrates the importance of measuring components at use condition.
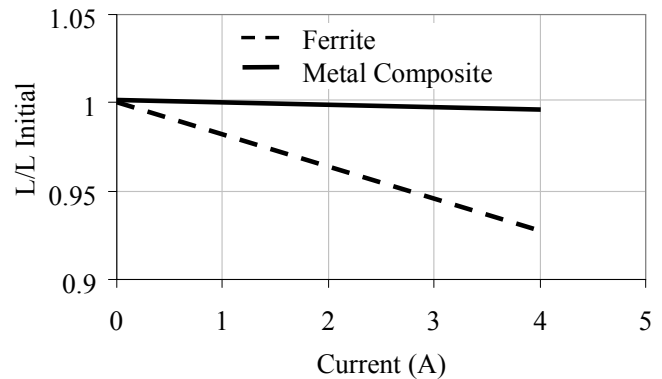

Figure 16. Summary of inductance change with current

CONCLUSIONS

This paper examined aspects of characterization needed to fully comprehend component behavior in order to provide a cost optimized solution for today's ultrahigh performance microprocessors. A description was provided of measurements using a commonly available system, the Agilent® 8753 Network Analyzer. A method to deembed the measurement fixture contribution was discussed. Higher order models were presented for both capacitors and inductors to address the shortcomings of simple models. This paper presented the need for measurements at use condition and illustrated a comparison between capacitors measured under use condition for various suppliers. Finally, several options of inductors were evaluated for performance over frequency and current.

ACKNOWLEDGMENTS

6

Copyright © 2011 by ASME

REFERENCES

[1] Wojewoda, L. E.; Hill, M. J.; Radhakrishnan, K.; Goyal, N.; "Use Condition Characterization of MLCCs, IEEE Transactions on Advanced Packaging," Vol. 32, Issue 1, February 2009.

[2] Piper, J., 1994, "Some Electrical Characteristics of Thin Dielectric (Low Voltage) MLCs," Kemet, USA. http://www.kemet.com/feedback&RequestType=Literatu re

[3] Eichorn, T., "Estimate Inductor Losses Easily in Power Supply Designs," Power Electronics Technology, pp. 14-24, April 2005

[4] Yu, Q.; Holmes, T. W.; Naishadham, K., "RF Equivalent Circuit Modeling of Ferrite-Core Inductors and Characterization of Core Materials," IEEE Transactions of Electromagnetic Compatibility, vol 44, pp. 258 -262 , Feb 2002.

[5] Kim, S.; Neikirk, D.P.; "Compact Equivalent Circuit Model for the Skin Effect," Microwave Symposium Digest, 1996., IEEE MTT-S International, vol 3, pp. 1815 – 1818, June 1996.

[6] Crane, L., 2006, "Ferrite and Powder Core Materials for Power Inductors," Coilcraft, http://www.inductors.ru/pdf/Doc496_Ferrite&Powder_C ore_Power_Inductors.pdf

[7] Maloy, S., 1999, "What is the Capacitance of This Capacitor?," TDK Components USA, http://www.tdk.com/pdf/whatisthecapofthiscap.pdf

[8] Wojewoda, L. E.; Hill, M. J., "Measurements and Modeling of Microprocessor Decoupling Capacitors," DesignCon, Santa Clara, CA, USA, 2005, TecForum TF7.

[9] Novak, I.; Miller, J. R., "Frequency-Dependent Characterization of Bulk and Ceramic Bypass Capacitors", presented at the 12th Topical Meeting on Electrical Performance of Electronic Packaging, Princeton, NJ, USA, October 2003.

[10] Sullivan, C. R; Kerm, A. M., "Capacitors With Fast Current Switching Require Distributed Models", presented at the Power Electronics Specialists Conference, June 17-21 2001.

[11] Smith, L. D.; Hockanson, D.; Kothari, K., "A Transmission-Line Model for Ceramic Capacitors for CAD Tools Based on Measured Parameters", presented at Electronic Components and Technology Conference, 2002, pp. 331-336.

[12] Randall, M.; Skamser, D.; Kinard, T.; Qazi, J.; Tajuddin, Aziz, "Thin Film MLCC," presented at CARTS USA, Albuquerque, NM, USA, March 26–29, 2007, Paper 6.6.

[13] Koripella, C. R. 1992, "Dielectrics Beyond Barium Titanate". Kemet. Greenville, SC USA. http://www.kemet.com/feedback&RequestType=Literatu re

[14] Pozar, D. M., *Microwave Engineering, 3rd Edition*. Hoboken, NJ USA: McGraw-Hill Professional Book Group, 1997.

[15] Harper, C. A., *Passive Electronic Component Handbook*. Blacklick, OH USA: John Wiley & Sons, Inc, 2005.

Copyright © 2011 by ASME